Nano Energy 128 (2024) 109929

Contents lists available at ScienceDirect

Nano Energy

journal homepage: www.elsevier.com/locate/nanoen

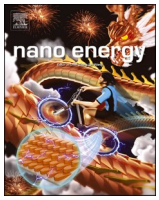

Full paper

Hybridized triboelectric-electromagnetic nanogenerators for efficient harvesting of wave energy for self-powered ocean buoy☆

Chengzhuo Zhang [a,b,1], Shaohui Yang [b,1], Xianggang Dai [c,d,1], Yongqiang Tu [b,1], Zhichang Du [b], Xiaobo Wu [c,d], Yan Huang [b], Jianyu Fan [b], Zhanyong Hong [a,c,d,*], Tao Jiang [a,c,d,*], Zhong Lin Wang [a,c,*]

[a] Guangzhou Institute of Blue Energy, Knowledge City, Huangpu District, Guangzhou 510555, PR China
[b] College of Marine Equipment and Mechanical Engineering, Jimei University, Xiamen 361021, PR China
[c] Beijing Key Laboratory of Micro-Nano Energy and Sensor, Center for High-Entropy Energy and Systems, Beijing Institute of Nanoenergy and Nanosystems, Chinese Academy of Sciences, Beijing 101400, PR China
[d] School of Nanoscience and Engineering, University of Chinese Academy of Sciences, Beijing 100049, PR China

ARTICLE INFO

Keywords:
Triboelectric nanogenerators
Hybrid nanogenerator
Oscillating water column
Marine Internet of Things

ABSTRACT

Triboelectric nanogenerators (TENGs) have been widely used in energy harvesting from low-frequency, irregular motions due to their unique characteristics and excellent electromechanical conversion efficiency. Harvesting ocean energy to build a marine Internet of Things (MIoTs) has become an important research field for TENGs. However, the output power density of TENGs must be further enhanced for promoting their practical applications, by effective means such as the coupling of TENGs and electromagnetic generators (EMGs). Herein, we report a triboelectric-electromagnetic hybrid nanogenerator (TEH-NG) for self-powered ocean buoy to harvest water wave energy efficiently for the first time. The buoy consists of a self-engineered wave energy converter for converting wave energy into simple turbomachinery energy through the pressure difference created by the relative motion, and a TEH-NG for converting the turbomachinery energy into electrical energy. The TENG delivers an average output power of 3.40 mW (with power density of 141.7 W m^{-3}), and the EMG achieves an average power of 0.04 W (with power density of 400.0 W m^{-3}). The excellent performance of the TEH-NG makes it a potential candidate for constructing the MIoTs to achieve distributed marine environmental monitoring networks.

1. Introduction

The development of renewable energy has become a hotly discussed topic as global energy demand continues to grow [1]. Among various types of renewable energy sources, water wave energy has become a hot research topic due to its wide distribution, relative predictability, and stability [2,3]. How to efficiently develop wave energy and build the marine Internet of Things (MIoTs) has become an important part of ocean energy utilization and marine environment monitoring [2,4]. However, compared with traditional land-based IoTs, the power supply of MIoTs sensor nodes faces huge challenges [5]. Currently, integrating wave energy harvesting technology into buoys to make them self-powered sensor nodes is the most feasible option for ocean energy harvesting [6].

Traditional wave energy harvesting relies on a combination of large mechanical floats and an electromagnetic generator (EMG) [7,8]. But it is difficult for conventional devices to effectively convert wave energy and transmit electricity to the power grid due to the low frequency and disordered nature of water wave energy [9]. The invention of triboelectric nanogenerator (TENG) offers a disruptive technology to harvest energy from the surrounding environment [5,10,11]. However, its high capacitive impedance limits its output power density, so traditional

☆ "Prof Zhong Lin Wang, an author on this paper, is the Editor-in-Chief of Nano Energy, but he had no involvement in the peer review process used to assess this work submitted to Nano Energy. This paper was assessed, and the corresponding peer review managed by Professor Chenguo Hu, also an Associate Editor in Nano Energy"

* Corresponding authors at: Guangzhou Institute of Blue Energy, Knowledge City, Huangpu District, Guangzhou 510555, PR China.
E-mail addresses: hongzhanyong@binn.cas.cn (Z. Hong), jiangtao@binn.cas.cn (T. Jiang), zhong.wang@mse.gatech.edu (Z.L. Wang).

[1] Chengzhuo Zhang, Shaohui Yang, Xianggang Dai and Yongqiang Tu contributed equally to this work.

https://doi.org/10.1016/j.nanoen.2024.109929
Received 17 May 2024; Received in revised form 13 June 2024; Accepted 24 June 2024
Available online 26 June 2024

single-mode TENG has begun to gradually transform into multi-mode TENG to achieve more efficient energy harvesting and conversion by integrating multiple electromechanical energy harvesting methods [12,13]. The excellent performance characteristics of oscillating water column TENG (OWC-TENG) were demonstrated [14]. By combining this technology with EMG, a hybridized system can be designed to increase the energy output [15]. This synergy will exploit the kinetic energy obtained by the OWC system through the natural motion of the waves and complement the reliable power generation capabilities of the electromagnetic principle, thereby improving the overall performance of power conversion [16,17]. This composite design takes full advantage of the respective strengths of both technologies and is expected to make significant progress in high-entropy energy [18,19].

The paper designs a triboelectric-electromagnetic hybrid nanogenerator (TEH-NG) for self-powered ocean buoys. The electrical output performance of TENG and EMG with different structural parameters is systematically investigated, and the optimal excitation conditions for the two generators at different wave frequencies and wave heights are tested [20]. Finally, to address the impedance mismatch problem, a triboelectric-electromagnetic power management circuit is constructed to improve charging efficiency [21]. Experimental results demonstrate that the TEH-NG can generate more output power than a single TENG and EMG, and can power wireless Bluetooth systems [22], significantly reducing the maintenance cost of the MIoTs [23], thus achieving important advances in the field of ocean energy utilization and environmental monitoring [24–26].

2. Results and discussion

2.1. Structural design and functional principles

The buoy can be used as a sensor node in the MIoTs (Fig. 1a). The energy collection and conversion of the device is driven by the float. The float drives the internal air through the up and down movement of sea water, causing changes in the internal pressure, which in turn causes the internal device (turbine) to generate electrical energy. The structure of the buoy consists of a central float, a downward heave plate and an upper turbine. And it is fixed to the sea surface through four moorings. As shown in Fig. S1 (Supporting Information), the part of the float immersed in the water is open. The relative motion between the waves and the float can be used to compress the air into high-pressure air and blow the turbine at high speed through a pipe in the middle of the float. At the same time, the unique design of the turbine guide vanes allows the rotor to pivot efficiently in the oscillating water flow (Fig. 1b).

The entire structure of the power generation unit is encased in a resin casing, which protects the internal components, and controls and directs the fluid while the turbine generates electricity, as shown in Fig. 1c. The power generation part consists of 2 modules, including a TENG module and an EMG module. The specific parts are shown in Fig. 1d. For the TENG module, a layered triboelectric approach is adopted, with four fan-blade shaped fluorinated ethylene propylene (FEP) layers radially adhered to the rotor disc, and on the stator disc, copper electrodes with a complementary pattern to the FEP layers on the rotor disc are coated on an acrylic plate using a printed circuit board (PCB) process. And a nylon layer is applied to the

copper electrodes to increase charge transfer. To reduce friction and increase the service life of the device, a non-contact friction method is used. Four rectangular grooves are evenly cut out of the rotor disc, and then four strips of rabbit furs with the same shape are pasted at the grooves. The selection of rabbit fur brushes as a kind of electropositive material with high fur density and surface charge density can largely reduce the materials wear and increase the device durability without decreasing the electrical outputs [11,27]. Fig. S2 compares the surface morphologies of FEP and nylon films before and after the tests, demonstrating that rabbit fur brushes can be used to reduce wear. For the EMG module, the rotor consists of an acrylic plate with a groove and four magnets with the same magnetic properties, while the stator consists of four coils with an inner diameter of 2 mm and an outer diameter of 20 mm fixed in the groove. The rotor of the TENG module and the EMG module are fixed on top of the same rotor of the turbine to ensure their synergy, so that the EMG and TENG are well coupled together to improve the utilization of wave energy.

Fig. 1e presents the schematic operating cycle of TENG and EMG. As the turbine rotor disc rotates, the magnets begin to cut the coils. According to Faraday's law of electromagnetic induction, the magnetic field changes during the cutting process, generating an induced electromotive force in the coils, thereby generating an induced current. Meanwhile, after the rabbit furs rub against the FEP film, the free charges on the electrodes are redistributed between the two electrodes through the load by electrostatic induction, balancing the changes in potential difference, thereby generating alternating current (AC).

2.2. Electrical characterization of TEH-NG module in wind tunnel

To obtain more accurate experimental results of TEH-NG outputs on the wind turbine, as shown in Fig. S3, an experimental wind tunnel that is consistent with the fluid generated by the oscillation of the floating body was designed through simulations. The turbulence flow generated by the fan is rectified into a laminar flow by combining honeycombs and filters. The relationship between the outputs of the TENG and the clearance at the wind speed of 2.5 m s^{-1} was first explored using four magnets, as illustrated in Fig. 2a. When the clearance between the rotor and stator is shortened to 0.7 mm, the open-circuit voltage, short-circuit current, and transferred charge of the TENG are 521.4 V, 15.9 μA, and 184.6 nC, respectively (Fig. S4). Theoretically, further narrowing the clearance could increase the open-circuit voltage and transferred charge. However, due to processing and installation tolerance, the rotor and stator may directly contact with each other at too small gap, hence reducing the rotational speed and current, accelerating the degree of material wear (Fig. S5). The relationship between the start-up wind speed of the turbine rotor and the clearance was further tested afterward as shown in Fig. 2b, where the required start-up wind speed gradually decreases from 2.6 m s^{-1} to 1.7 m s^{-1} with the gradual increase of the clearance. To reduce the clearance to improve output performance, and also pursue lower starting wind speeds, we ultimately chose the 0.7 mm clearance instead of the 0.4 mm clearance by a comprehensive consideration.

Wind speed has a significant effect on the outputs of the TENG. Fig. 2c and S6 show the variations of the open-circuit voltage, short-circuit current, and transferred charge of the TENG at a wind speed of 3.1 m s^{-1} with a load of four magnets. The peak open-circuit voltage is 545.4 V, the peak short-circuit current is 23.4 μA, and the peak transferred charge is 195.2 nC. It can be seen from Fig. 2d-e and S7, that as the wind speed increases, the voltage, current, and charge all increase gradually. Fig. S8 shows the variation of open-circuit voltage, short-circuit current, and transferred charge of TENG at different wind speeds with loads of 6 and 8 magnets. It is found that the outputs of the TENG decrease with the increase in the number of magnets due to the increase in the mass of the rotor, resulting in a decrease in the rotational speed (Fig. 2g-h). Fig. 2f and S9 show that the peak output power of TENG equipped with different numbers of magnets first increases and then decreases with the increase of the external resistance at different wind speeds, and the maximum peak power is 11.05 mW. The matched resistance is around 50 MΩ and the peak output power is proportional to the wind speed and inversely proportional to the number of magnets (Fig. 2i).

Under the same conditions, the EMG performance was tested as shown in Fig. 3a and S10. The outputs of the EMG increase as the distance between the rotor and stator gets closer at a wind speed of 2.5 m s^{-1}. At the distance of 3.5 mm, the open-circuit voltage, short-circuit current, and transferred charge are 8.2 V, 153.7 mA, and 992.3 μC. With the shortening of clearance from 7.5 mm to 2.0 mm, the start-

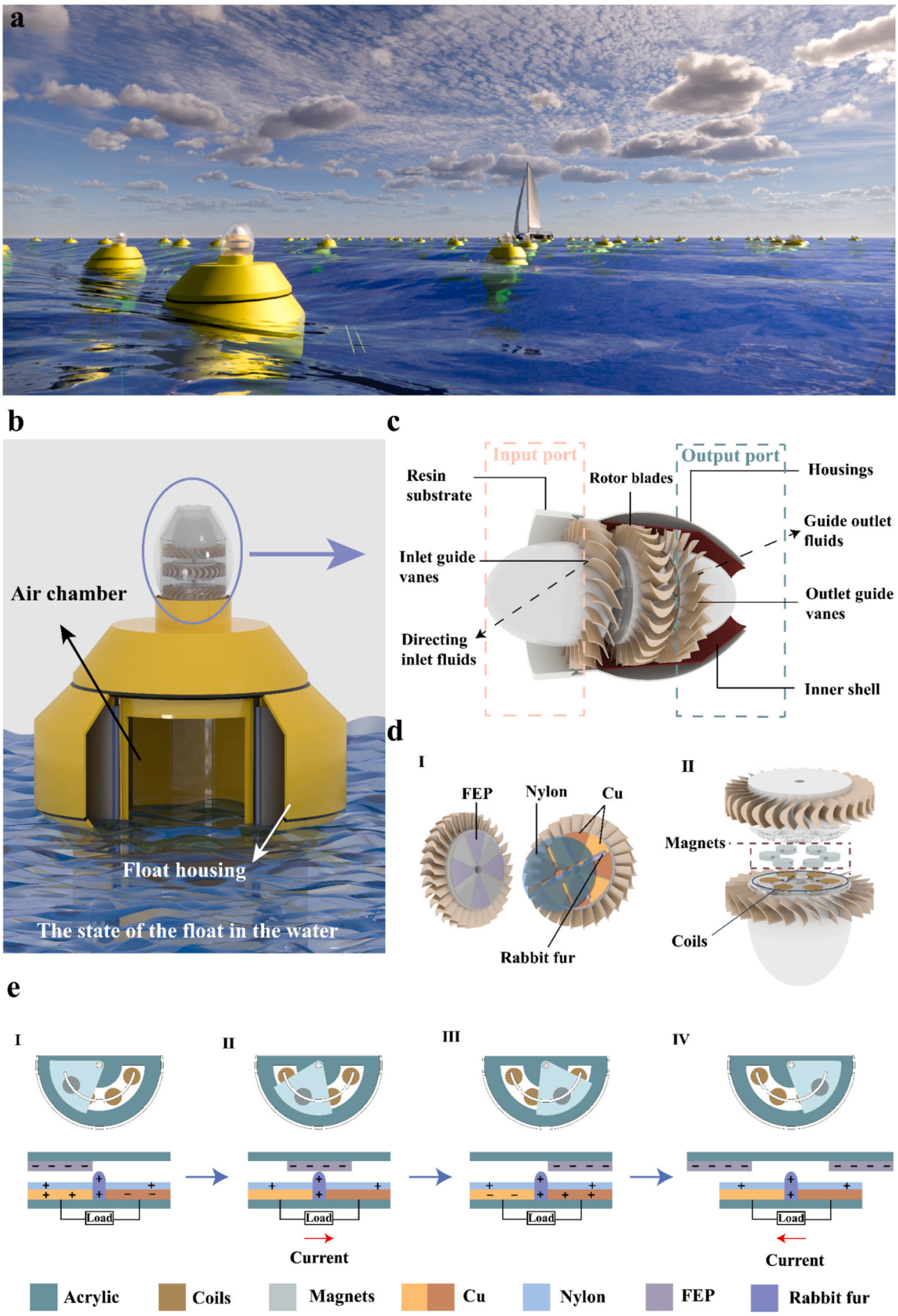

Fig. 1. Wave energy collection and working principle of the ocean buoy. a) Schematic diagram of a series of sensor nodes for MIoTs. b) Schematic internal structure of the buoy. c) Structural diagram of the turbine. d) Structural details of the stator and rotor discs for turbines. e) Working principle diagram of the TENG and EMG.

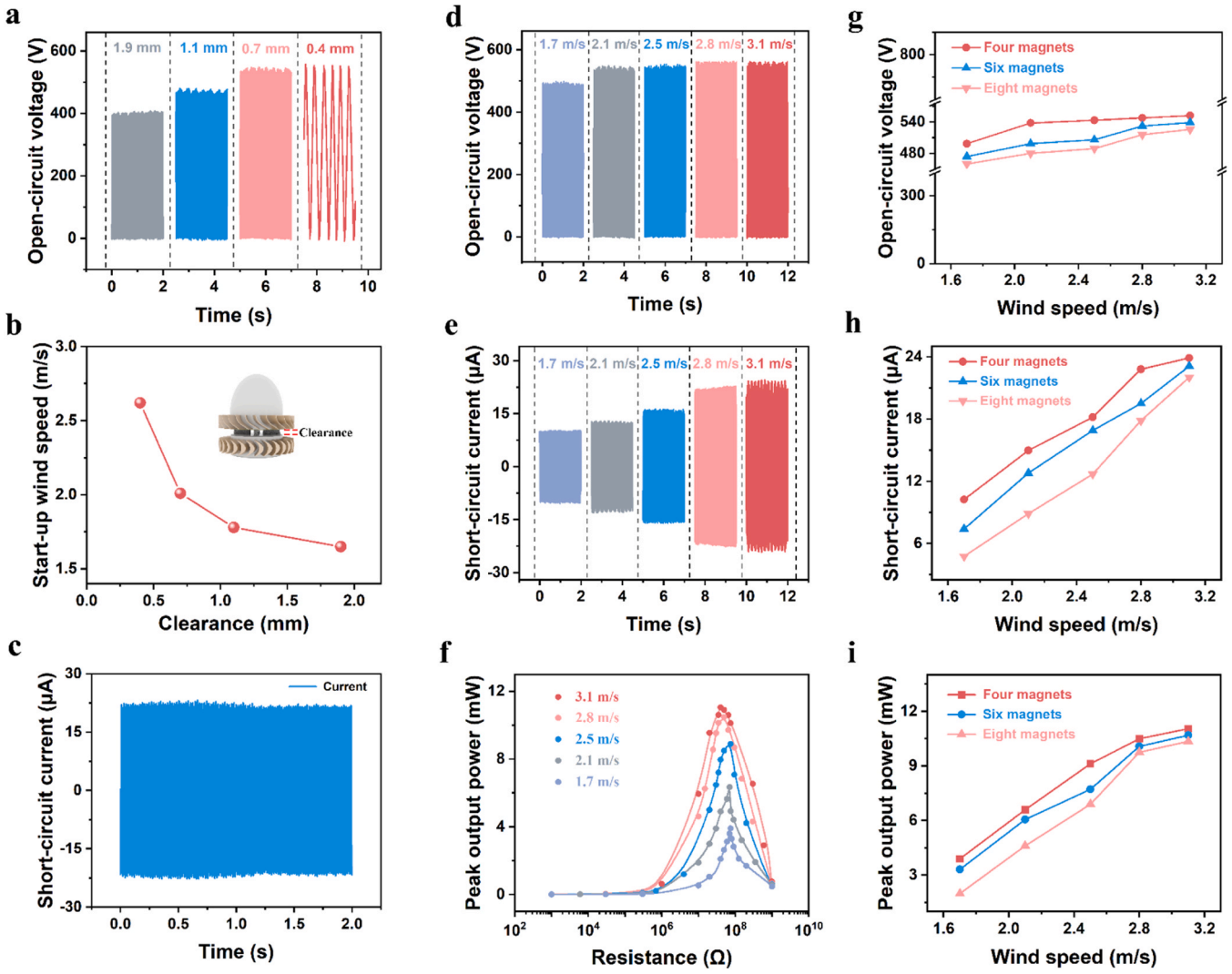

Fig. 2. Output characteristics of TENG in wind tunnel. a) Relationship between the generated open-circuit voltage and the clearance between TENG rotor and stator with 4 magnets. b) Relationship between the rotor-stator clearance of the TENG with 4 magnets and the start-up wind speed. c) Short-circuit current of TENG with 4 magnets at a wind speed of 3.1 m s^{-1}. d) Open-circuit voltage, e) short-circuit current, and f) peak output power of the TENG with 4 magnets at different wind speeds. g) Open-circuit voltage, h) short-circuit current, and i) peak output power of TENG with different numbers of magnets at different wind speeds.

up wind speed gradually increases from 2.1 m s^{-1} to 3.3 m s^{-1}. The increase in the starting wind speed with the decrease of clearance is because of the increased pressure drop of air through the turbine, and a larger wind speed is required to overcome the greater pressure drop for the turbine to start. To enable the rotor to start at low wind speed, the clearance for EMG was selected to be 3.5 mm.

Fig. 3c and S11 show that the open-circuit voltage, short-circuit current, and transferred charge of the EMG with four magnets are 13.6 V, 202.5 mA, and 809.6 μC at a wind speed of 3.1 m s^{-1}. The variations of voltage, current, and charge of EMG with respect to the wind speed are shown in Fig. 3d-e, and S12. It can be found that the outputs of EMG have a similar pattern to those of TENG, that is, the open-circuit voltage and short-circuit current of EMG are proportional to the wind speed, while the transferred charge is not affected by the wind speed and is only related to the magnetic flux. As the number of magnets increases, the rotational speed decreases at the same wind speed, and the open-circuit voltage and short-circuit current decrease (Fig. 3g-h). Also the transferred charge decreases (Fig. S13), because the increase in the magnet number affects the magnetic flux density.

Fig. 3f and S14 illustrate the peak output power of the EMG set with respect to the wind speed for different numbers of magnets. The peak output power also shows a trend of first increasing and then decreasing as the resistance of the external resistor increases, while the peak output power increases with the increase of wind speed (Fig. 3i). The maximum peak output power is 0.33 W. But the peak power at the same wind speed decreases gradually as the number of magnets increases.

2.3. Electrical characterization of TEH-NG module in water waves

Experimental tests revealed that the output performances of TENG and EMG decrease as the number of magnets increases, so we selected 4 magnets as their optimal structural parameters. The outputs of the TEH-NG were then tested under different water wave excitations using a wave pool to simulate real wave conditions, as shown in Fig. 4a-b, and S15-S16. The maximum open-circuit voltage, short-circuit current, and transferred charge were all measured at a period of 1.2 s and a wave height of 0.25 m. As shown in Fig. 4c-d and S17, under the optimal excitation conditions, the open-circuit voltages of the TENG and EMG are 351.8 V and 10.3 V, respectively. And the short-circuit currents are 22.4 μA and 142.5 mA, respectively, while the transferred charges are 184.5 nC and 809.2 μC. The clearance of 0.7 mm exhibits the lowest wear compared to the previous clearance of 0.4 mm after 300, 000 working cycles (Fig. 4e) and the attenuation of short-circuit current is only 5.4 % (Fig. S18). The TEH-NG has been proved to be more suitable

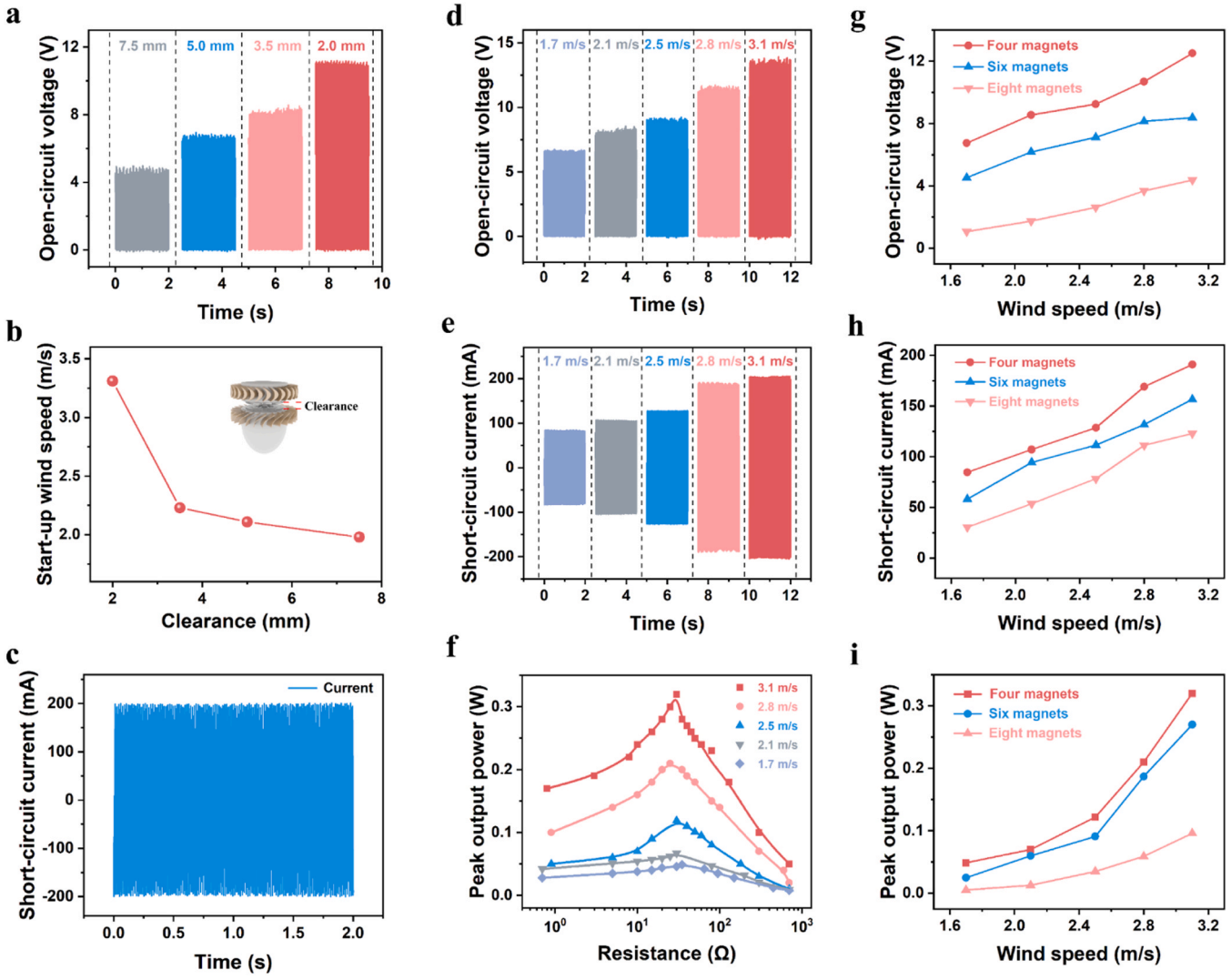

Fig. 3. Output characteristics of the EMG in a wind tunnel. a) Relationship between the open-circuit voltage and the EMG rotor-stator clearance with 4 magnets. b) Relationship between the EMG rotor-stator clearance and the start-up wind speed. c) Short-circuit current of EMG with 4 magnets at a wind speed of 3.1 m s^{-1}. d) Open-circuit voltage, e) short-circuit current, and f) peak power of EMG with 4 magnets at different wind speeds. g) Open-circuit voltage, h) short-circuit current, and i) peak power of EMG with different numbers of magnets at different wind speeds.

for harvesting water wave energy under low frequency and low amplitude conditions.

For further evaluating the actual output performance of the TEH-NG in water waves, the peak/average output powers and volume power densities of the TEH-NG were tested as shown in Fig. 5a-b and S19. The peak output power of TENG under optimal water wave excitation is 10.60 mW with a peak volume power density of 419.2 W m^{-3}, which delivers an average power of 3.40 mW and an average power density of 141.7 W m^{-3}. The EMG has a peak power of 0.11 W, a peak power density of 1100.0 W m^{-3}, an average power of 0.04 W, and an average power density of 400.0 W m^{-3}. The power densities of the device have significant enhancements based on our previous work about the OWC-TENG, further verifying the superiority of the air turbine structure [28]. The coupling of the TENG and EMG can increase the overall energy conversion efficiency and electrical outputs. The hybrid device can capture and convert the water wave energy over a wider frequency range, which is also suitable for both large and small vibrations. This hybrid device has a relatively simple structure, with less dependence on topography, and can be selected offshore, nearshore or onshore. It has no underwater moving parts and is highly reliable, which can be developed in composite with offshore structures and reduce engineering costs.

Fig. 5c shows the power management circuit of the TEH-NG for harvesting ocean energy, which can be connected to both TENG and EMG simultaneously. The TENG and EMG complement each other in the mid-frequency band, which can better cover the collection of wave energy from low to high frequencies, providing a more reliable energy collection and supply system, and solving the problem that relatively high energy-consuming sensors cannot be powered. The charging curves of the TEH-NG to various capacitors after passing through the power management circuit are illustrated in Fig. 5d-e. As can be seen, the EMG can charge a 1000 μF capacitor to 4.8 V within 13.4 s, while the TENG requires 40.8 s. When the capacitance decreases, the charging time for reaching 4.8 V decreases. For the TEH-NG, it only requires 5.1 s to charge the 1000 μF capacitor to 4.8 V, showing that the charging effect of the hybridized nanogenerator far exceeds that of the single power module, which proves that the TEH-NG has great potential for ocean energy collection. Then the TEH-NG was used to charge a storage capacitor (C_s) to power an anemometer, as shown in Fig. 5f and Video S1. The capacitor of 2 mF is charged to 5.0 V in 11 s and then the switch is turned on, successfully driving the anemometer uninterruptedly. Furthermore, the TEH-NG can light up 112 light-emitting diodes (LEDs),

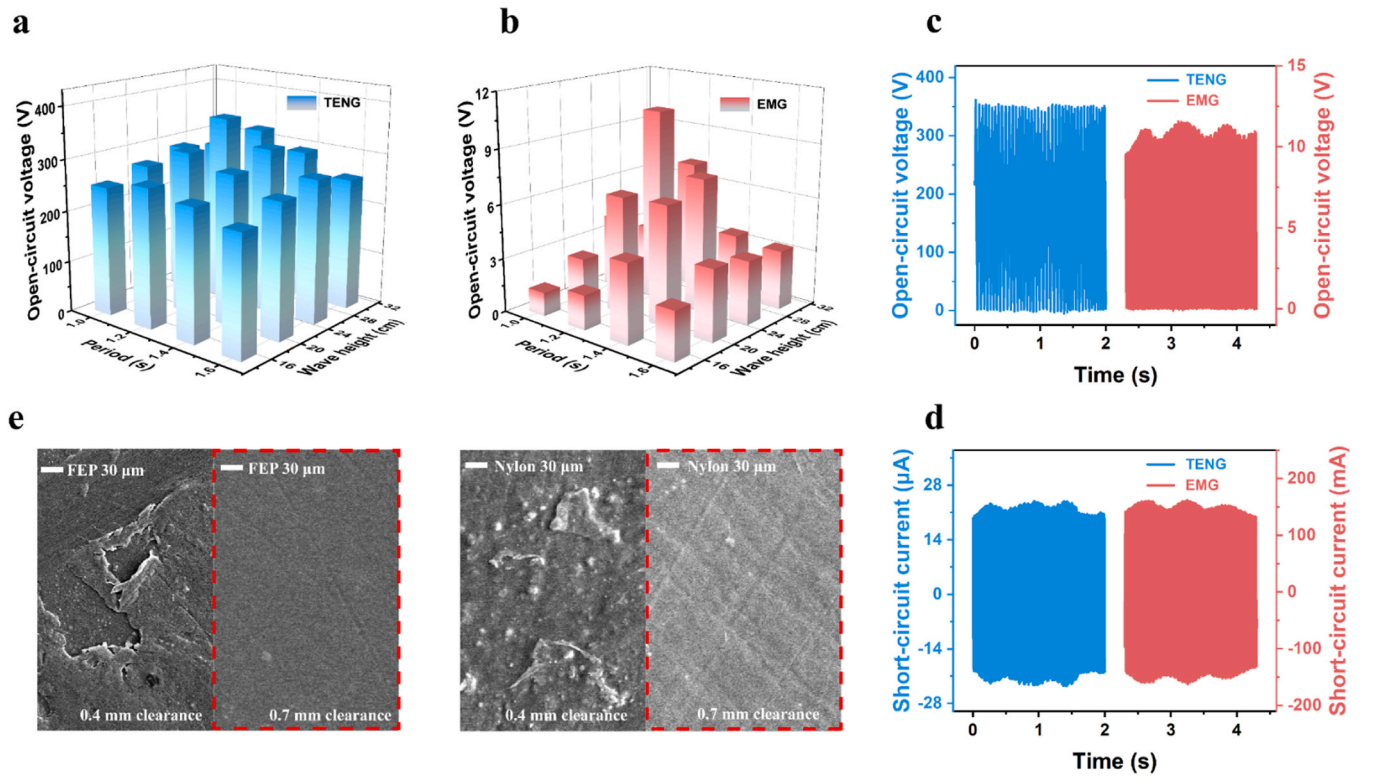

Fig. 4. Output characteristics of the TEH-NG in water waves. a, b) Open-circuit voltages of TENG and EMG under different water wave excitations. c, d) Comparison of open-circuit voltage and short-circuit current between TENG and EMG under optimal water wave excitations. e) Comparative chart of the wear degree of FEP and nylon membranes at different clearances.

as shown in Fig. S20. After the above experiments, it is directly verified that the device can successfully collect low-frequency wave energy and generate electricity continuously. Detailed photograph of the developed system is shown in Fig. S21.

Supplementary material related to this article can be found online at doi:10.1016/j.nanoen.2024.109929.

2.4. Self-powered marine monitoring sensor for the Internet of Things based on TEH-NG

The TENG can achieve high voltage output, but its output current is small, which makes its practical applications very limited, but the hybridization by the EMG improves the electrical performance. Therefore, to verify the feasibility of the designed generator, its practical application was demonstrated as shown in Fig. 6. The collection of marine data and the sending and receiving of signals are processed through a network control with remote access, as illustrated in Fig. 6a, where the microcontroller is connected to the data collection terminal through a wireless Bluetooth module.

A photograph of the technical setup used for the interactivity application is illustrated in Fig. 6b, comprising of 3 components: (i) electronic device, (ii) management circuit, and (iii) generator. The pH and temperature sensors are connected to the generator through a management circuit, which charges a 0.33 F capacitor, and takes roughly 220 s to reach 5.0 V. After that, the circuit starts and sends the detected pH and temperature information to the mobile via a wireless Bluetooth module in 3 s to achieve the monitoring of seawater condition, as shown in Fig. 6c and Video S2. The experimental results and data demonstrate the high potential of TEH-NG to play a key role in the development of sustainable and efficient ocean energy harvesting technologies. The TEH-NG is capable of stably converting mechanical energy, such as wave energy, into electrical energy to provide the necessary energy for marine equipments in complex and variable marine environments by combining triboelectric and electromagnetic power generation methods. Particularly in the field of self-powered MIoTs buoys, the TEH-NGs not only reduce dependence on conventional energy sources, maintenance costs and the need for energy replenishment, but also enable continuous operation of real-time data collection and communication for remote sensor networks.

Supplementary material related to this article can be found online at doi:10.1016/j.nanoen.2024.109929.

3. Conclusion

The purpose of this paper is to design and investigate a self-powered energy harvesting system for offshore sensor buoys. The TENG module and EMG module are combined in one generator, making the two complementary, which significantly increases the output power and can power some high-power consumption sensors. The turbine's inertial energy storage mechanism can store and accumulate the discrete ocean energy to ensure that the rotor can rotate for a long period, which makes the TEH-NG have superior low-frequency output performance and durability. The combination of the non-contact mode TENG and the parallel connection of EMG under the structural parameter of 4 magnets was finally confirmed after a series of experimental comparisons. The TEH-NG performance was also tested under different water wave excitations, and it was found that the device has the maximum outputs under a water wave excitation with a period of 1.2 s and a wave height of 0.25 m. The average output power of its TENG module is 3.40 mW (141.7 W m^{-3}) and the average output power of EMG is 0.04 W (400.0 W m^{-3}). Furthermore, the device successfully powered the operation of pH and temperature sensors as well as Bluetooth transmission under low-frequency water wave excitation. The experimental results above prove the feasibility of this energy collection system in the MIoTs to achieve real-time monitoring, collection, transmission, and processing of data on the marine environment, marine resources, and

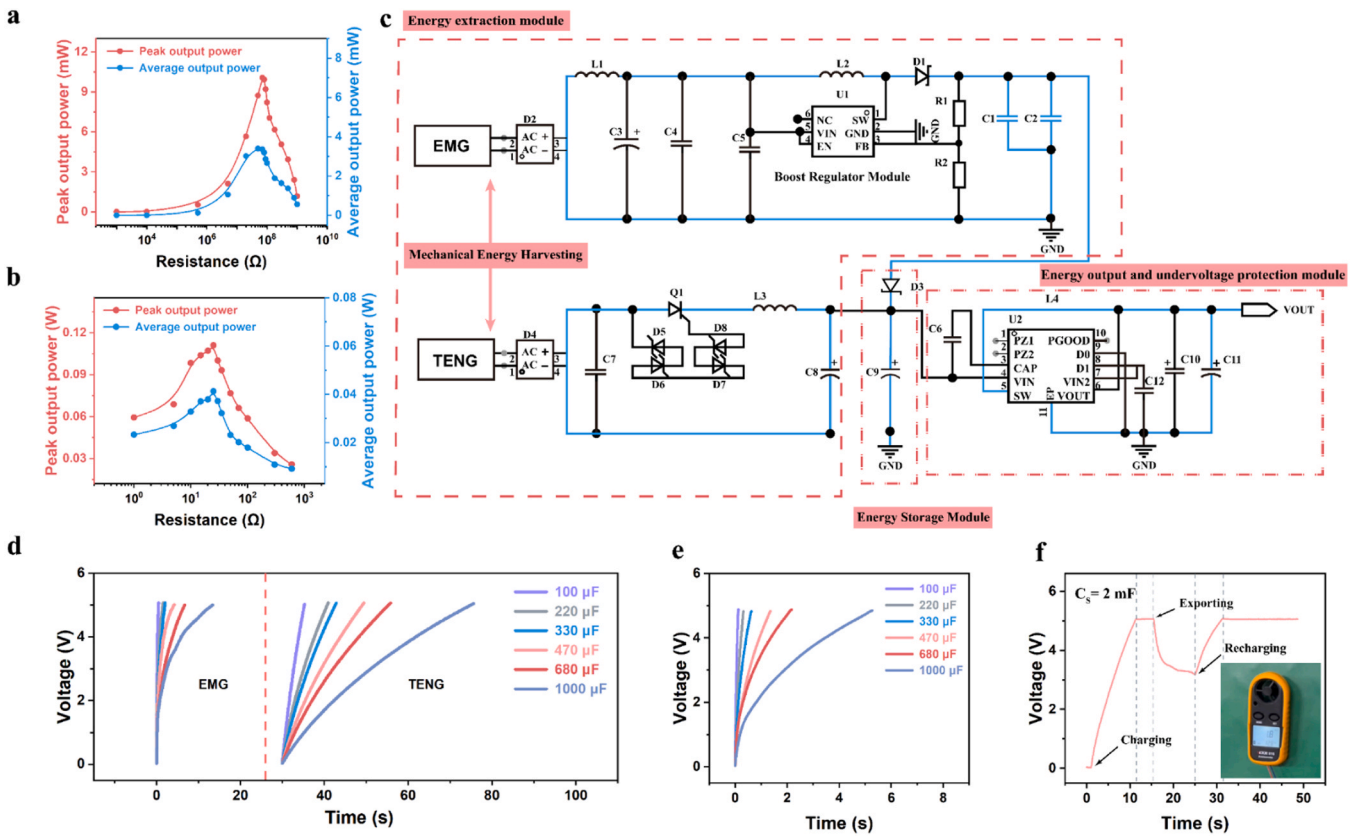

Fig. 5. Power management performance of the TEH-NG in water waves. a, b) Peak output power and average output power of TENG and EMG under optimal water wave excitation conditions. c) Power management circuit for the TENG and EMG. d) Charging curves of capacitors by the TENG and EMG, respectively. e) Charging curves of the capacitors by the TEH-NG. f) Charging curve of the TEH-NG to a capacitor of 2 mF for powering an anemometer in water waves.

marine facilities, thus enhancing the capacity of marine environmental protection, resource development, and utilization.

Experimental

Fabrication of buoy device

Float Fabrication: the float is an aluminum alloy sleeve-shaped shell with a height of 0.6 m and a radius of 0.3 m. The shell consists of an inner wall (0.003 m thick), an outer wall (0.005 m thick), and a closed hollow sandwich located between the inner and outer walls, which was used to provide buoyancy to keep the whole device floating on the water surface. The interior of the float is a hollow structure with a 0.1 m radius hole at one end for fixing the power generator and a 3 mm thick pendant plate at the other end for increasing the pendant motion of the float.

TENG Fabrication: for the rotor disc, a laser cutting machine was used to cut a 2 mm thick acrylic plate into a circle with an inner diameter of 7 mm and an outer diameter of 51 mm, on which 4 pieces of radially aligned fan-shaped FEP film with a thickness of about 25 μm were adhered. To create the stator disc, PCB engraving technology was employed to carve a Cu electrode plate with 8 grids. The dimensions and shape of the stator disc are identical to those of the rotor disc. On the Cu electrode disc, four rectangular grooves with a width of 4 mm and a length of 32 mm were cut out, and four strips of rabbit furs with a length of about 4 mm were pasted inside the grooves. Finally, on the surface of the Cu electrode, a layer of 30 μm thick nylon was applied.

EMG Fabrication: for the rotor, first of all, a laser cutting machine was used to cut a 6 mm thick acrylic plate into 4, 6, 8 circular grooves with a depth of 5 mm and a radius of 1 mm, evenly cut around the center of the circle on the top. All magnets inside have their N poles facing upwards in the circular grooves to ensure that the polarity is the same. For the stator disc, the same number of circular grooves of the same size and shape were cut on a 3 mm acrylic plate by a laser cutter, and the same number of coils with a thickness of 2 mm and a wire diameter of 0.1 mm are fixed in the grooves.

Turbine Fabrication: the model structure of the turbine was designed in SolidWorks software, and its mechanical structure was printed by a 3D printer. The TENG and EMG were fixed on the turbine, the rotor of the turbine rotated around a central axis with a radius of 4 mm, and an acrylic shell with an inner diameter of 71 mm and an outer diameter of 75 mm was installed outside the turbine.

Experimental instrumentation

Experimental Procedure and Measurement Equipments: electrical properties were tested using a Keithley 6514 system electrometer, a large wave pool, an anemometer, and images of the surfaces of the FEP film and nylon film were tested using a SU8020 Cold Field Scanning Electron Microscope.

Author contributions

C.Z., S.Y. and Z.H. conceived the idea. Z.H., T.J. and Z.L.W. conducted the work and supervised the experiments. C.Z., S.Y, Z.H., T.J. and Z.L.W. prepared the manuscript. C.Z., S.Y., X.D. and Y.T. designed and fabricated the device and performed the electrical measurements. Z.D., X.W., Y.H., and J.F. helped for the electrical measurements and application demonstrations. All the authors discussed the results and commented on the manuscript.

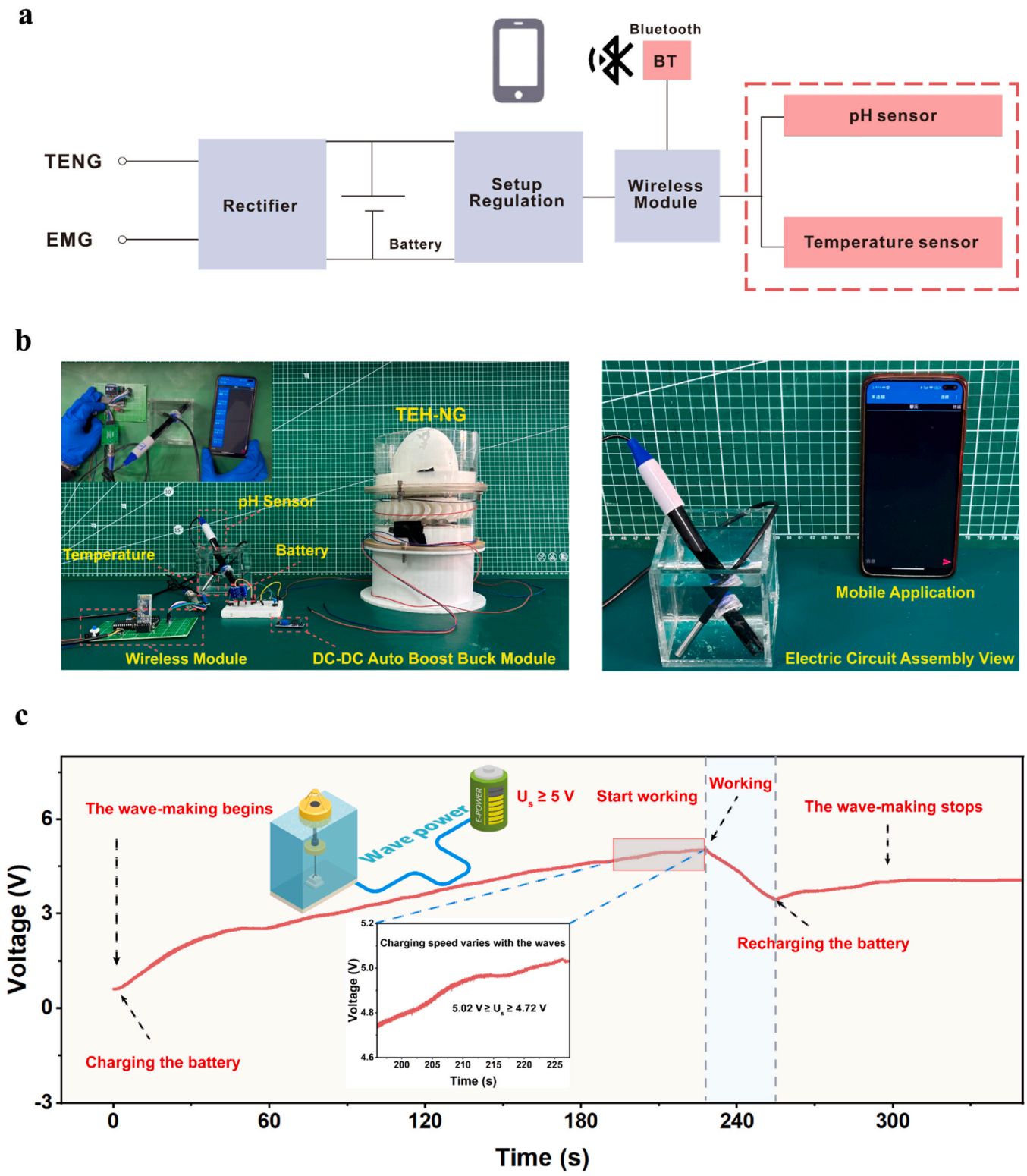

Fig. 6. Applications of the TEH-NG for monitoring and sensing in MIoTs. a) Schematic diagram of signal transmission from the buoy sensor node. b) Left: Different components in the assembly of the TEH-NG including a wireless Bluetooth module, a battery, a pH sensor, a temperature sensor, a DC-DC boost module, and the TEH-NG. Right: pH and temperature sensors and a mobile phone. c) Charging diagram of the TEH-NG to a battery for powering the pH and temperature sensing system under the water wave excitations.

CRediT authorship contribution statement

Jianyu Fan: Visualization, Methodology. **Xiaobo Wu:** Methodology, Investigation. **Yan Huang:** Visualization, Methodology, Investigation. **Yongqiang Tu:** Methodology, Investigation. **Zhichang Du:** Methodology, Investigation. **Shaohui Yang:** Writing – original draft, Methodology, Investigation. **Xianggang Dai:** Writing – original draft, Methodology, Investigation. **Zhong Lin Wang:** Writing – review & editing, Supervision. **Chengzhuo Zhang:** Writing – original draft, Methodology, Investigation, Conceptualization. **Zhanyong Hong:**

Writing – review & editing, Supervision, Investigation, Conceptualization. **Tao Jiang:** Writing – review & editing, Supervision, Methodology, Investigation.

Declaration of Competing Interest

The authors declare that they have no known competing financial interests or personal relationships that could have appeared to influence the work reported in this paper.

Data Availability

Data will be made available on request.

Acknowledgements

C.Z., S.Y., X.D. and Y.T. contributed equally to this work. The research was supported by the National Key R & D Project from Minister of Science and Technology (2021YFA1201601, 2021YFA1201603), Industry-University Cooperation Project in Fujian Province University (2023H61010068), Fujian Provincial Natural Science Youth Funding (022J05155), Xiamen Science and Technology Bureau Nature Funding (3502Z20227057), Beijing Nova Program (20220484036), and Innovation Project of Ocean Science and Technology (22–3–3-hygg-18-hy).

Appendix A. Supporting information

Supplementary data associated with this article can be found in the online version at doi:10.1016/j.nanoen.2024.109929.

References

[1] P.J. Jeff Scruggs, Harvesting ocean wave energy, Scienece 323 (2009) 1176–1178.
[2] G. Zhu, J. Chen, T. Zhang, Q. Jing, Z.L. Wang, Radial-arrayed rotary electrification for high performance triboelectric generator, Nat. Commun. 5 (2014) 3426.
[3] I. Gonçalves, C. Rodrigues, J. Ventura, Sea state adaptation enhances power output of triboelectric nanogenerators for tailored ocean wave energy harvesting, Adv. Energy Mater. 14 (2023) 2302627.
[4] H. Joe, H. Roh, H. Cho, S.-C. Yu, Development of a flap-type mooring-less wave energy harvesting system for sensor buoy, Energy 133 (2017) 851–863.
[5] C. Chen, Z. Wen, J. Shi, X. Jian, P. Li, J.T.W. Yeow, X. Sun, Micro triboelectric ultrasonic device for acoustic energy transfer and signal communication, Nat. Commun. 11 (2020) 4143.
[6] Z. Wen, H. Guo, Y. Zi, M.H. Yeh, X. Wang, J. Deng, J. Wang, S. Li, C. Hu, L. Zhu, Z. L. Wang, Harvesting broad frequency band blue energy by a triboelectric-electromagnetic hybrid nanogenerator, ACS Nano 10 (2016) 6526–6534.
[7] Z. Wu, H. Guo, W. Ding, Y.C. Wang, L. Zhang, Z.L. Wang, A hybridized triboelectric-electromagnetic water wave energy harvester based on a magnetic sphere, ACS Nano 13 (2019) 2349–2356.
[8] H. Hong, X. Yang, H. Cui, D. Zheng, H. Wen, R. Huang, L. Liu, J. Duan, Q. Tang, Self-powered seesaw structured spherical buoys based on a hybrid triboelectric–electromagnetic nanogenerator for sea surface wireless positioning. Energy Environ. Sci. 15 (2022) 621–632.
[9] S.-F. Leung, H.-C. Fu, M. Zhang, A.H. Hassan, T. Jiang, K.N. Salama, Z.L. Wang, J.-H. He, Blue energy fuels: converting ocean wave energy to carbon-based liquid fuels via co2 reduction, Energy Environ. Sci. 13 (2020) 1300–1308.
[10] X. Han, Y. Ji, L. Wu, Y. Xia, C.R. Bowen, Y. Yang, Coupling enhancement of a flexible bifeo3 film-based nanogenerator for simultaneously scavenging light and vibration energies, Nano-micro Lett. 14 (2022) 198.
[11] S. Gao, H. Wei, J. Wang, X. Luo, R. Wang, Y. Chen, M. Xiang, X. Chen, H. Xie, S. Feng, Self-powered system by a suspension structure-based triboelectric-electromagnetic-piezoelectric hybrid generator for unifying wind energy and vibration harvesting with vibration attenuation function, Nano Energy 122 (2024) 109323.
[12] L. Long, W. Liu, Z. Wang, W. He, G. Li, Q. Tang, H. Guo, X. Pu, Y. Liu, C. Hu, High performance floating self-excited sliding triboelectric nanogenerator for micro mechanical energy harvesting, Nat. Commun. 12 (2021) 4689.
[13] Z. Xu, L. Chen, Z. Zhang, J. Han, P. Chen, Z. Hong, T. Jiang, Z.L. Wang, Durable roller-based swing-structured triboelectric nanogenerator for water wave energy harvesting, Small 20 (2023) 2307288.
[14] Z.L. Wang, Triboelectric nanogenerators as new energy technology and self-powered sensors – principles, problems and perspectives, Faraday Discuss. 176 (2014) 447–458.
[15] C. Xu, X. Wang, Z.L. Wang, Nanowire structured hybrid cell for concurrently scavenging solar and mechanical energies, J. Am. Chem. Soc. 131 (2009) 5866–5872.
[16] Y. Luo, P. Chen, L.N.Y. Cao, Z. Xu, Y. Wu, G. He, T. Jiang, Z.L. Wang, Durability improvement of breeze-driven triboelectric-electromagnetic hybrid nanogenerator by a travel-controlled approach, Adv. Funct. Mater. 32 (2022) 2205710.
[17] C. Zhang, W. Yuan, B. Zhang, O. Yang, Y. Liu, L. He, J. Wang, Z.L. Wang, High space efficiency hybrid nanogenerators for effective water wave energy harvesting, Adv. Funct. Mater. 32 (2022) 2111775.
[18] X. Fu, S. Xu, Y. Gao, X. Zhang, G. Liu, H. Zhou, Y. Lv, C. Zhang, Z.L. Wang, Breeze-wind-energy-powered autonomous wireless anemometer based on rolling contact-electrification, ACS Energy Lett. 6 (2021) 2343–2350.
[19] C. Han, Z. Cao, Z. Yuan, Z. Zhang, X. Huo, L. a Zhang, Z. Wu, Z.L. Wang, Hybrid triboelectric-electromagnetic nanogenerator with a double-sided fluff and double halbach array for wave energy harvesting, Adv. Funct. Mater. 32 (2022) 2205011.
[20] H. Zhao, M. Xu, M. Shu, J. An, W. Ding, X. Liu, S. Wang, C. Zhao, H. Yu, H. Wang, C. Wang, X. Fu, X. Pan, G. Xie, Z.L. Wang, Underwater wireless communication via teng-generated maxwell's displacement current, Nat. Commun. 13 (2022) 3325.
[21] X. Zhang, M. Yu, Z. Ma, H. Ouyang, Y. Zou, S.L. Zhang, H. Niu, X. Pan, M. Xu, Z. Li, Z.L. Wang, Self-powered distributed water level sensors based on liquid–solid triboelectric nanogenerators for ship draft detecting, Adv. Funct. Mater. 29 (2019) 1900327.
[22] J. An, Z. Wang, T. Jiang, P. Chen, X. Liang, J. Shao, J. Nie, M. Xu, Z.L. Wang, Reliable mechatronic indicator for self-powered liquid sensing toward smart manufacture and safe transportation, Mater. Today 41 (2020) 10–20.
[23] S. Zhang, Z. Jing, X. Wang, K. Fan, H. Zhao, Z.L. Wang, T. Cheng, Enhancing low-velocity water flow energy harvesting of triboelectric–electromagnetic generator via biomimetic-fin strategy and swing-rotation mechanism. ACS Energy Lett. 7 (2022) 4282–4289.
[24] B. Zhao, Z. Li, X. Liao, L. Qiao, Y. Li, S. Dong, Z. Zhang, B. Zhang, A heaving point absorber-based ocean wave energy convertor hybridizing a multilayered soft-brush cylindrical triboelectric generator and an electromagnetic generator, Nano Energy 89 (2021) 106381.
[25] Y. Zhong, H. Zhao, Y. Guo, P. Rui, S. Shi, W. Zhang, Y. Liao, P. Wang, Z.L. Wang, An easily assembled electromagnetic-triboelectric hybrid nanogenerator driven by magnetic coupling for fluid energy harvesting and self-powered flow monitoring in a smart home/city, Adv. Mater. Technol. 4 (2019) 1900741.
[26] X. Fu, Y. Qin, Z. Zhang, G. Liu, J. Cao, B. Fan, Z. Wang, Z. Wang, C. Zhang, Ultra-robust and high-performance rotational triboelectric nanogenerator by bearing charge pumping. Energy Environ. Mater. 7 (2023) 12566.
[27] P. Chen, J. An, S. Shu, R. Cheng, J. Nie, T. Jiang, Z.L. Wang, Super-durable, low-wear, and high-performance fur-brush triboelectric nanogenerator for wind and water energy harvesting for smart agriculture, Adv. Energy Mater. 11 (2021) 2003066.
[28] S. Yang, C. Zhang, Z. Du, Y. Tu, X. Dai, Y. Huang, J. Fan, Z. Hong, T. Jiang, Z. L. Wang, Fluid oscillation-driven bi-directional air turbine triboelectric nanogenerator for ocean wave energy harvesting, Adv. Energy Mater. 14 (2024) 2304184.

Chengzhuo Zhang is currently a postgraduate student at Jimei University. He is currently under joint training at Beijing Institute of Nanoenergy and Systems, Chinese Academy of Sciences. He will graduate in 2025. His research interests are in the area of micro and nano energy harvesting and utilization, self-powered sensors, and high efficiency energy storage technology for triboelectric nanogenerators.

Shaohui Yang received his Master's degree and Ph.D. degree in Electrical Engineering and Automation from China Agricultural University, Beijing, China in 2001 and 2006, respectively. He is currently a Professor at Jimei University. His current research interests include marine power generation equipment and ocean monitoring instruments.

Xianggang Dai is Ph.D. candidate in the School of Nanoscience and Engineering at University of Chinese Academy of Sciences, Beijing, China. His current research focuses on ocean blue energy harvesting and conversion, self-powered system applications and hydrogen production from triboelectric nanogenerator self-powered electrolyzed water.

Yongqiang Tu received his Ph.D. degree in Precision instruments and machinery from Beihang University, Beijing, China in 2023. He also received Ph.D. degree in Industrial engineering from Arts et Mtiers, France in 2024. He is currently an Associate Professor at Jimei University. His current research interests include marine power generation equipment and ocean monitoring instruments.

Zhichang Du received his bachelor's degree from The Xi'an Jiao Tong University in 2014. He also received Ph.D. degree in Mechanical Engineering from Tsinghua University in 2020. He is currently an Associate Professor at Jimei University. His research focuses on marine power generation equipment, fluid control, and ocean monitoring instruments.

Xiaobo Wu received his PhD degree from the Department of Materials Science and Engineering at Northwestern Polytechnical University in 2022, and is currently a postdoctoral researcher at Beijing Institute of Nanoenergy and Nanosystems, Chinese Academy of Sciences. His research interests include photocatalysis, solar cells, TENG and energy harvesting devices, focusing on the application of TENG in blue ocean energy.

Yan Huang received his B.S. degree in Computer Science Engineering from Xiamen University TKK college in China. He received his M.S degree in Software Engineering in 2014 from the University of Leicester in Britain. He currently received his Ph.D. in Vehicle Operation Engineering from the State Key Laboratory of Traction Power of Southwest Jiaotong University in China in 2020. His is current a lecturer in the school of mechanical and energy engineering of Jimei University in China. His research interests cover the fields of Nonstationary Signal Processing, Wave Energy Converting and Control Technology.

Jianyu Fan received his Ph.D. degree in Mechatronics from Xidian University, Xi'an, China in 2019. He is currently a Lecturer at Jimei University. His current research interests are focused on ocean energy harvesters.

Prof. Zhanyong Hong is a professor at Beijing Institute of Nanoenergy and Nanosystems, Chinese Academy of Sciences. His main research interests are the device structure and performance optimization of triboelectric nanogenerators for water wave energy harvesting, TENG network design and optimization, energy management and storage, self-powered marine Internet of Things system, and offshore hybrid energy development and application.

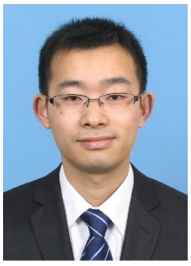

Dr. Tao Jiang is a professor at Beijing Institute of Nanoenergy and Nanosystems, Chinese Academy of Sciences. He received his B.S. and Ph.D. degrees from School of Materials Science and Engineering, in 2008 and 2014, respectively, from East China University of Science and Technology. After graduation, he worked in the Beijing Institute of Nanoenergy and Nanosystems as a postdoctoral research fellow. His research interests are the theoretical studies of triboelectric nanogenerators, and practical applications in blue energy harvesting.

Prof. Zhong Lin Wang received his Ph.D. degree from Arizona State University in physics. He now is the Hightower Chair in Materials Science and Engineering, Regents' Professor at Georgia Tech, the chief scientist and director of the Beijing Institute of Nanoenergy and Nanosystems, Chinese Academy of Sciences. Prof. Wang has made original and innovative contributions to the synthesis, discovery, characterization and understanding of fundamental physical properties of oxide nanobelts and nanowires, as well as applications of nanowires in energy sciences, electronics, optoelectronics and biological science. His discovery and breakthroughs in developing nanogenerators establish the principle and technological road map for harvesting mechanical energy from environmental and biological systems for powering personal electronics. His research on self-powered nanosystems has inspired the worldwide efforts in academia and industry for studying energy for micro-nano-systems, which is now a distinct disciplinary in energy research and future sensor networks. He coined and pioneered the fields of piezotronics and piezophototronics by introducing piezoelectric potential gated charge transport process in fabricating new electronic and optoelectronic devices.